

Interfacial Tension-Mediated Droplet Fusion in Rectangular Microchannels

Jongin Hong^{1,2}, Minsuk Choi³,
Andrew J. deMello¹ & Joshua B. Edel^{1,2}

¹Department of Chemistry, Imperial College London,
South Kensington Campus, London SW7 2AZ, UK

²Institute of Biomedical Engineering, Imperial College London,
South Kensington Campus, London SW7 2AZ, UK

³Department of Mechanical Engineering, Imperial College London,
South Kensington Campus, London SW7 2AZ, UK

Correspondence and requests for materials should be addressed
to J.B. Edel (joshua.edel@imperial.ac.uk) and A.J. deMello
(a.demello@imperial.ac.uk)

Accepted 24 July 2009

Abstract

We successfully demonstrate the merging of aqueous droplets within a microfluidic channel mediated by a difference in interfacial tension. Interfacial tension is shown to have a significant influence on the hydrodynamic forces associated with a segmented flow in a rectangular microchannel and results in the possibility of merging multiple droplets in a simple fashion. This facility is important in allowing droplet-based microfluidic systems to be used as synthetic tools in complex reaction processing.

Keywords: Droplet-based microfluidics, Droplet fusion, Interfacial tension, Polydimethylsiloxane (PDMS), Ferrofluid

Introduction

Over the last decade, microfluidic systems have developed into a valuable instrumental platform for performing chemistry and biology^{1,2}. More recently, particular attention has been focused on using droplet-based microfluidic systems as a fundamental tool in high-throughput experimentation²⁻⁶. It has been shown that instabilities between immiscible flows in microfluidic networks enable the generation of highly monodisperse, picoliter-volume droplets of variable composition in an immiscible carrier fluid. Such encapsulated droplets can be used to mimic artificial cells or isolated reaction vessels. Compared to conventional single-phase microfluidic systems, the localization of reagents within discrete and isolated compartments is considered to be an extremely effective way of both

enhancing reaction yields for mixing and mass transfer limited reactions and narrowing residence time distributions associated with the transport of material in continuous flows^{3,4,6}. Such microdroplets can also be fused, subdivided, sorted, isolated or incubated to multi-functional analytical devices⁶. Importantly, the ability to controllably merge droplets containing different reagents is crucial when performing complex chemical or biological reactions or kinetic studies of chemical and biological substances. Merging allows the precise mixing of reagents at a fixed position in both time and space. Recently, several active and passive techniques have been developed to merge droplets in microfluidic networks. Active merging of droplets has been achieved by electrofusion induced by AC or DC potentials^{7,8}, optical tweezers and vortex traps⁹ and heating¹⁰. However, such approaches require the incorporation of either active components in a device or complicated external infrastructure. In contrast, passive fusion of multiple droplets has been achieved by modifying droplet size¹¹, geometric modification of the core microfluidic structure¹²⁻¹⁴ and local modification of the surface properties of channel walls¹⁵. In all these approaches, three key processes must occur: a) the velocities of the two (or more) droplets are reduced, b) drainage of the continuous phase between adjacent droplets brings droplets into close proximity and c) droplet coalescence occurs by the connecting droplet interfaces subsequent to rupturing of the thin film between the droplets. Unfortunately, the removal of the continuous phase often requires the incorporation of complex microstructures. In this article, we demonstrate a novel approach for passively merging droplets in a rectangular microchannel, which is mediated simply by differences in the interfacial tension between adjacent droplets. This approach drastically simplifies merging of droplets in many situations.

Results and Discussion

The merging of droplets, in our approach, can be conceptualized as follows. A segmented flow in a circular microchannel (such as a capillary) behaves as a tight-fitting piston (Figure 1a) and thus the segmented flow and carrier fluid move at approximately the same speed. However, a segmented flow in a rectangular (or square) channel (most commonly seen in poly-

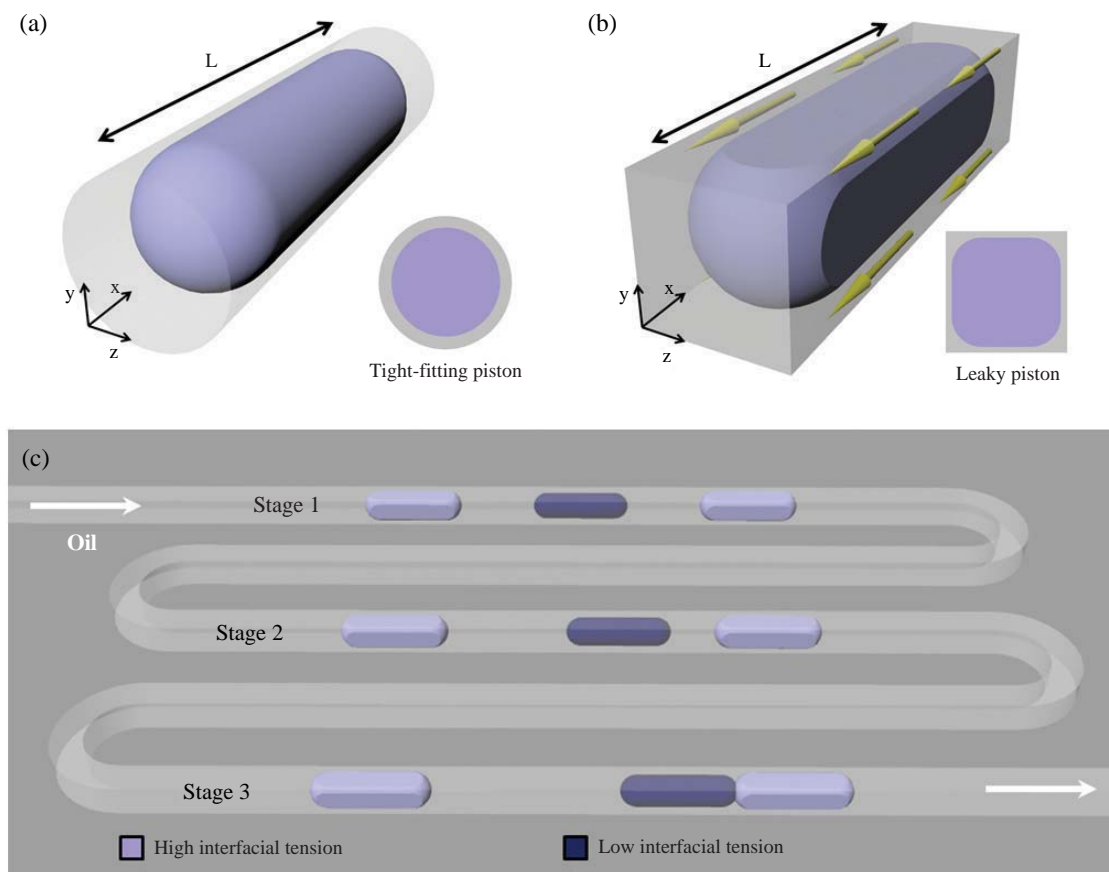


Figure 1. Illustrations of (a) a droplet in a circular microchannel (a tight fitting piston), (b) a droplet in a rectangular microchannel (a leaky piston), and (c) interfacial tension-mediated droplet fusion.

dimethylsiloxane (PDMS)-based microfluidic systems) behaves like a leaky piston. In this case, the carrier fluid can bypass the segmented flow through 'leaky' corners (Figure 1b). The area of the carrier fluid-filled corners is directly related to capillary number and includes a contribution from the interfacial tension between the two immiscible fluids¹⁶. Total non-dimensional fluid flow (Q_T) is composed of the corner flow (Q_1) and the plug flow pushing the droplet (Q_2). According to Wong *et al.*¹⁶, the non-dimensional fluid flow can be expressed as

$$Q_T = |Q_1 + Q_2| = \frac{\kappa C_D}{AL} Ca^{-1/3} + A \quad (1)$$

where κ is a constant that depends only on the corner geometry, C_D is a constant relating to total drag, A is the area of the static plug and L is the dimensionless length of a plug. An average fluid velocity can be obtained by dividing Q_T by the capillary area A_c .

$$V = \frac{c_1}{L} Ca^{-1/3} + c_2 \quad (2)$$

In the case where $L \gg Ca^{-1/3}$ (i.e. when a droplet is sufficiently long), the corner flow is negligible and the total fluid flow is similar to the plug flow. Here L is the dimensionless length of a plug and Ca is the capillary number (equal to $\mu U/\sigma$, where μ is the viscosity of the carrier fluid and σ is the interfacial tension between two immiscible phases). In the case where $1 \ll L \ll Ca^{-1/3}$ (i.e. the plug is moderately long), the fluid in the corner is much faster than the droplet and the value of c_2 is negligible. For two droplets with different properties and the fixed average fluid velocity, the velocity ratio between the two droplets can be obtained from Equation (2) and is given by,

$$\frac{U_1}{U_2} = \left(\frac{L_1}{L_2} \right)^{3/2} \left(\frac{\sigma_2}{\sigma_1} \right)^{1/2} \quad (3)$$

where U_i , L_i and σ_i are the velocity, length and the interfacial tension of a plug i , respectively. Equation (3) implies that a droplet with longer length and smaller interfacial surface tension will move at a higher velocity.

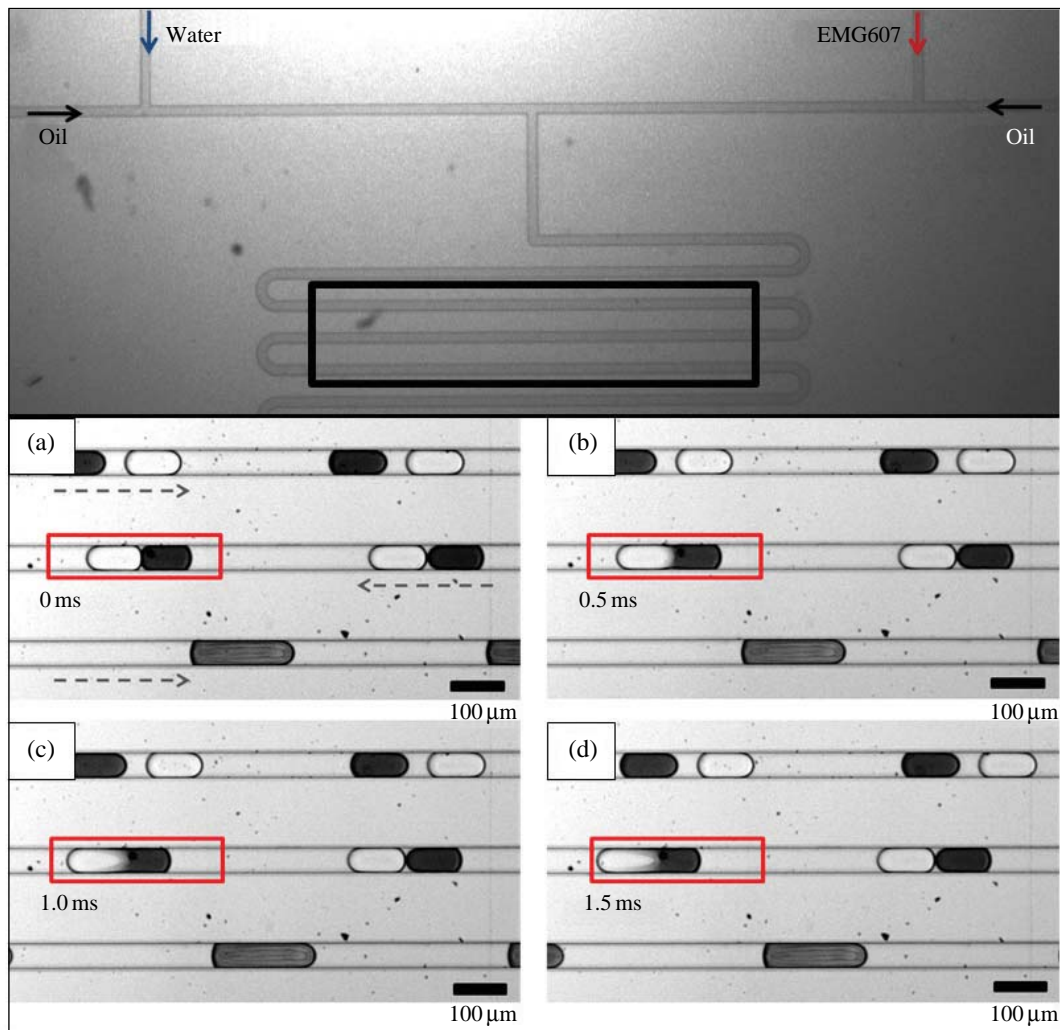


Figure 2. A time sequence of interfacial tension-mediated droplet fusion as low interfacial tension droplets approach high interfacial droplets: (a) 0 ms, (b) 0.5 ms, (c) 1.0 ms and 1.5 ms (Scale bar: 100 μm).

Table 1. Fluidic properties of water and ferrofluid (EMG 607).

	Surface tension (mN/m)	Interfacial tension (mN/m)*	Density (g/cm ³)	Viscosity (mPa · s)
Water	72.80	18.69 ± 2.38	1.0	1.005
EMG 607	39.77 ± 1.35	7.01 ± 1.01	1.13	2
FC oil	14.75 ± 0.05	—	1.82	1.4
FC oil with PFO	13.98 ± 0.21	—	1.80	1.4

*Interfacial tension between a FC oil with PFO and water (or EMG 607)

Inspection of equation 3 suggest that that longer and lower interfacial tension droplets will move at higher velocities. A scenario for interfacial tension-mediated droplet fusion is presented in Figure 1. First, stable and alternating droplets of two (or more) sets of aqueous solutions with different interfacial tensions are formed

and introduced into a rectangular microchannel (stage 1). A low interfacial tension droplet will subsequently approach a droplet with high interfacial tension because of the difference in corner flows (stage 2). This is then followed by physical contact between the two droplets and initiation of the merging process (stage 3).

In order to verify the proof-of-concept of the interfacial tension-mediated droplet fusion, alternating droplets were generated using a double T-junction channel and an oil-to-water ratio of 5 : 2 in PDMS microfluidic devices. Droplet lengths were matched at 115 μm to remove the influence of droplet size on droplet velocities. Figure 2 shows the time sequence of droplet pairs passing through a winding microchannel 2.5 mm in length. These sequential images clearly illustrate the primary results of this study. As can be seen, the low interfacial tension droplet (EMG 607, black) moves progressively closer to the high interfacial tension droplet (water, transparent) due to the difference in the corner flow of the carrier fluid and causes drainage of the carrier fluid. The detailed fluidic properties of water and EMG607 are summarized in Table 1. Through image analysis, the velocities of water and EMG-607 droplets are found to be 44.03 ± 0.06 and 45.23 ± 0.04 mm/s, respectively. After physical contact between the two droplets, the interface is disturbed via drop deformation and merging can occur. Importantly, the marked droplet pair shows an evolution of the drop-

let coalescence process. Close views of the pair as it moves through the rectangular microchannel are shown in Figure 3. Dark images were processed by using a 5×5 Edge Hipass filter. After initiation of coalescence, most of the carrier fluid is drained within 1.0 ms and the interface between the two droplets disappears (Figure 3b). This is followed by the commencement of droplet mixing. Mixing in the droplet is laminar and convection driven. More detailed mixing patterns after the fusion will be explored by using fluorescence lifetime imaging¹⁷. Importantly, after droplet fusion, the merged droplet maintains a constant velocity. Table 2 summarizes droplet velocities at different flow conditions for two different droplets with identical sizes. These tabulated results confirm that EMG607 droplets (low interfacial tension) move at a higher velocity than water droplets (high interfacial tension).

Conclusions

We have successfully demonstrated droplet fusion within a simple microfluidic system using the concept of interfacial tension-mediated merging. We are currently exploring a variety of aqueous phases including organic and inorganic chemicals miscible with water, nanoparticle solutions and biological samples for fundamental studies and practical applications. We believe that the merging concept will find application in many areas of chemical and biological processing including use in complex biological assays and small molecule synthesis.

Table 2. Droplet velocities under different flow conditions.

Oil flow rate ($\mu\text{L}/\text{min}$)	V_{water} (mm/s)	V_{EMG607} (mm/s)
5.0	28.10 ± 0.04	28.86 ± 0.04
7.5	36.36 ± 0.07	37.38 ± 0.06
10	44.03 ± 0.06	45.23 ± 0.04
12.5	52.30 ± 0.04	55.35 ± 0.05
15.0	60.63 ± 0.04	64.32 ± 0.05

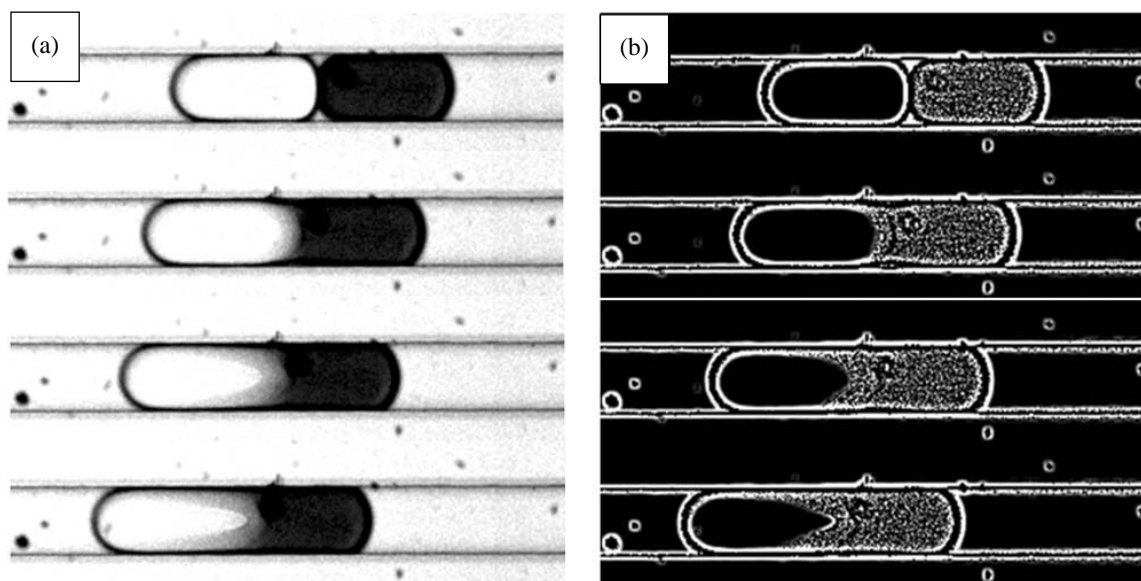


Figure 3. Close up view of a pair of droplets before and during the fusion process: (a) bright and (b) dark images.

Materials and Methods

Microfluidic devices were fabricated in PDMS, a transparent elastomer, using soft lithographic techniques¹⁸. PDMS base and curing agent (Sylgard 184; Dow Corning) were mixed in a ratio of 10 : 1 w/w, degassed and decanted onto an SU-8 master. The resulting structure was cured for 2 hours on a hot plate at 65°C and then peeled off from the master. After punching inlet and outlet holes through the structured PDMS layer, the layer was contacted to a partially cured PDMS slab and baked at 65°C for 6 hours to form the completed microdevice in an oven. The fluidic channels have a rectangular cross section of 50 × 50 μm and the length of a merging channel is sufficiently long so that droplets are merged after generation of alternating water and ferrofluid (EMG 607) droplets. A 10 : 1 (v/v) mixture of 3 M fluorinated FC-3283/EGC1700 and 1H, 1H, 2H, 2H-perfluorooctanol (PFO) was used as a carrier fluid for all experiments. EMG607 chosen as a model fluid in our study is a water-based ferrofluid containing magnetic nanoparticles of iron oxide coated with a cationic surfactant and purchased from Ferrotec (London, UK). Surface and interfacial tension measurements were obtained using a pendant drop measurement system (DSA100, Kruss GmbH) and a software for drop shape analysis (DSA3, Kruss GmbH). Precision syringe pumps (PHD 2000, Harvard Apparatus) were used to motivate fluids at a range of volumetric flow rates through the microchannels. A high speed camera (Phantom®, v649) was used for data acquisition and Matlab® used to analyze recorded images and calculate velocities.

Acknowledgements

This work was supported by the RCUK Basic Technology Programme. JH would like to acknowledge D. Holt (University of Cambridge) and J. Dane (Imperial College London) for assistance with bulk interfacial tension measurements.

References

1. deMello, A.J. Control and detection of chemical reactions in microfluidic systems. *Nature* **442**, 394-402 (2006).
2. Hong, J. Microfluidic systems for high throughput screening. *BioChip J.* **2**, 12-26 (2008).
3. Song, H., Chen, D.L. & Ismagilov, R.F. Reactions in droplets in microfluidic channels. *Angew. Chem. Int. Ed.* **45**, 7336-7356 (2006).
4. Gunther, A. & Jensen, K.F. Multiphase microfluidics: from flow characteristics to chemical and materials synthesis. *Lab. Chip* **6**, 1487-1503 (2006).
5. Huebner, A. *et al.* Microdroplets: a sea of applications? *Lab. Chip* **8**, 1244-1254 (2008).
6. Hong, J., Edel, J.B. & deMello, A.J. Micro- and nano-fluidic systems for high-throughput biological screening. *Drug Discovery Today* **14**, 134-146 (2009).
7. Priest, C., Herminghaus, S. & Seemann, R. Controlled electrocoalescence in microfluidics: targeting a single lamella. *Appl. Phys. Lett.* **89**, 134101(1-3) (2006).
8. Link, D.R. *et al.* Electric control of droplets in microfluidic devices. *Angew. Chem. Int. Ed.* **45**, 2556-2560 (2006).
9. Lorentz, R.M. Vortex-trap-induced fusion of femtoliter-volume aqueous droplets. *Anal. Chem.* **79**, 224-228 (2007).
10. Kohler, J.M. *et al.* Digital reaction technology by micro segmented flow-components, concepts and applications. *Chem. Eng. J.* **101**, 201-216 (2004).
11. Song, H., Tice, J.D. & Ismagilov, R.F. A microfluidic system for controlling reaction networks in time. *Angew. Chem. Int. Ed.* **42**, 768-772 (2003).
12. Tan, Y.-C., Ho, Y.L. & Lee, A.P. Droplet coalescence by geometrically mediated flow in microfluidic channels. *Microfluid. Nanofluid.* **3**, 495-499 (2007).
13. Bremond, N., Thiam, A.R. & Bibette, J. Decompressing emulsion droplets favors coalescence. *Phys. Rev. Lett.* **100**, 024501(1-4) (2008).
14. Niu, X., Gulati, S., Edel, J.B. & deMello, A.J. Pillar-induced droplet merging in microfluidic circuits. *Lab. Chip* **8**, 1837-1841 (2008).
15. Fidalgo, L.M., Abell, C. & Huck, W.T.S. Surface-induced droplet fusion in microfluidic devices. *Lab. Chip* **7**, 984-986 (2007).
16. Wong, H., Radke, C.J. & Morris, S. The motion of long bubbles in polygonal capillaries. Part 2. Drag, fluid pressure and fluid flow. *J. Fluid. Mech.* **292**, 95-110 (1995).
17. Srisa-Art, M., deMello, A.J. & Edel, J.B. Fluorescence lifetime imaging of mixing dynamics in continuous-flow microdroplet reactors. *Physical Review Letters* **101**, 014502(1-4) (2008).
18. Beard, N.R., Zhang, C.X. & deMello, A.J. In-column field-amplified sample stacking of biogenic amines on microfabricated electrophoresis devices. *Electrophoresis* **24**, 732-739 (2003).